SIMULATION OF PREMIXED COMBUSTION AND NEAR WALL FLAME QUENCHING IN SPARK IGNITION ENGINES WITH AN IMPROVED FORMULATION OF THE BRAY-MOSS-LIBBY MODEL

Ranasinghe C.P* and Malalasekera W.
*Author for correspondence
Wolfson School of Mechanical and Manufacturing Engineering,
Loughborough University,
Loughborough, Leicestershire, LE11 3TU,
UK.
E-mail : C.P.Ranasinghe@lboro.ac.uk

ABSTRACT

Theoretical and experimental based modifications have been investigated, such that the BML model can be applied to wall-bounded combustion modelling eliminating the wall flame acceleration problem. Estimation of integral length scale of turbulence has been made dynamic so that allowance for spatial inhomogeneity of turbulence is made. A new dynamic formulation has been proposed based on the Kolmogorov-Petrovski-Piskunov analysis and fractal geometry to evaluate the mean flame wrinkling scale. In addition, a novel empirical correlation to quantify the quenching rates in the influenced zone of the quenching region near solid boundaries has been derived based on experimentally estimated flame image data.

The proposed model was then applied to simulate the premixed combustion in spark ignition engines. Full cycle combustion in a Ricardo E6 engine for different operating conditions was simulated. Results show that the present improvements have been successful in eliminating the wall flame acceleration problem, while accurately predicting the in-cylinder pressure rise.

INTRODUCTION

Optimisation of combustion performances in Internal Combustion (IC) engines is of extensive research interest due to two key factors. First, it is the combustion process, which principally determines the engine performance. In-cylinder combustion is extremely complex and still not completely understood [1]. Second is the legislative requirements. With the demand of increasingly stringent emissions standards, engine manufacturers are faced with the challenging task of producing vehicles that abide by these regulations with increased power and efficiency.

The physical processes involved in the combustion chamber of IC engines are so complex and some phenomena may be hardly accessible to experimental investigations [2].

NOMENCLATURE

Letters and symbols

A_f	$[-]$	Flame surface area
$\bar{c}$	$[-]$	Mean progress variable
d	$[m]$	Distance from the solid boundary
D	$[-]$	Fractal dimension in three dimension
$\mathcal{D}$	$[-]$	Normalized quenching distance
Da	$[-]$	Damköhler number
I_0	$[-]$	Flame front wrinkling factor
k	$[m^2 s^{-2}]$	Turbulent kinetic energy
Ka	$[-]$	Karlovitz number
l_f	$[m]$	Active flamelet length
l_i	$[m]$	Integral length scale of turbulence
l_q	$[m]$	Quenched flamelet length
l_y	$[m]$	Flamelet wrinkling scale
p	$[Nm^{-2}]$	Pressure
Pe	$[-]$	Peclet Number
QR	$[-]$	Quenching rate
Re_t	$[-]$	Turbulent Reynolds number
Re_λ	$[-]$	Taylor Reynolds Number
S_l	$[ms^{-1}]$	Laminar burning velocity
S_t	$[ms^{-1}]$	Turbulent burning velocity
u'	$[ms^{-1}]$	Turbulent intensity
δ	$[m]$	Laminar flame thickness
ε	$[m^2 s^{-3}]$	Dissipation rate of turbulent kinetic energy
ν	$[m^2 s^{-1}]$	Kinematic viscosity
ρ	$[gm^{-3}]$	Mass density
Σ	$[m^{-1}]$	Flame surface density
τ	$[-]$	Heat release factor
ϕ	$[-]$	Fuel air equivalence ratio
$\bar{\omega}$	$[gm^{-3}s^{-1}]$	Unburned mass consumption rate
ϵ_0	$[m]$	Outer cut off scale
ϵ_i	$[m]$	Inner cut off scale

Subscripts

u	$[-]$	Unburned
cr	$[-]$	Critical
max	$[-]$	Maximum
in	$[-]$	Intake
$wall$	$[-]$	Near/On wall
Q	$[-]$	At quenching

The traditional routine of engine design follows manual engine modifications, excessive testing, and analysis of experimental results in order to optimize the combustion processes. This iterative process is profoundly slow, costly and imparts no way itself in identifying the optimum conditions. In present day research on this aspect, Computational Fluid Dynamics (CFD) simulations play a vital role and appear to be the best candidate for providing such a design tool that evaluates the future combustion technologies, with a shorter lead-time, avoiding difficult experimental investigations [2].

In the modelling literature of premixed charged Spark Ignition (SI) engine combustion, several models with varying degree of complexity are found. Eddy Brake-Up (EBU) [3,4] type and Flame Surface Density [5] (FSD) type are the well-established and widely used premixed combustion model types in present-day combustion studies. Even though the EBU type models have been used [6] in modelling engine combustion its use is limited due to the inherent problem of wall flame acceleration [7]. FSD approach also suffers from the same deficiency to a certain extent and some ad hoc measures are taken in both types of models to minimise the effects of this problem [7-9].

The well-known Bray-Moss-Libby [10] (BML) FSD model and its variants have been successfully used in premixed combustion modelling studies for many years. Application of the original BML model for the simulation of open-stagnation flames has shown to be capable of producing comparably good results when compared to other models. However, applications of the BML model in wall bound combustion problems are rare. This is due to the 'near wall flame acceleration problem', or in simple terms, predicting excessively higher unphysical reaction rates near solid boundaries. A number of alternative forms of the BML model have been suggested in the literature to overcome this problem, but most of them are based on ad-hoc assumptions.

In the present study, this inherent wall acceleration problem in BML type models is addressed via newly developed correlations, which provide the necessary allowance for the anisotropy in turbulence and thermal quenching near walls. Premixed combustion in SI engines is analysed as the immediate application of the novel formulation, as it is one of the most practically important cases of wall bounded premixed combustion. Moreover, the evaluation of several BML model constants has made dynamic here, so that only a single adjustable constant is left for fine-tuning.

BML FORMULATION OF FLAME SURFACE DENSITY

The mean unburned mass consumption rate $\bar{\omega}$ in FSD approach is expressed as;

$$\bar{\omega} = \rho_u \, I_0 S_l \Sigma \tag{1}$$

where, Σ is the flame surface density: the available flame surface area per unit volume. ρ_u is the unburned gas density and S_l is the unstretched laminar burning velocity. The factor I_0 accounts for the stretch and curvature effects of flamelets on the burning velocity.

In the BML formulation, the flame surface density is given by:

$$\Sigma = \frac{g\bar{c}(1-\bar{c})}{l_y} = \frac{g}{|\sigma_y|}\frac{\bar{c}(1-\bar{c})}{C_b l_i \left(\frac{S_l}{u'}\right)^n} \tag{2}$$

where, l_y is the integral scale of flame wrinkling and $\bar{c}$ is the mean progress variable of reaction. Formerly, σ_y was considered to be a universal constant having a value of 0.5. However, recent studies [11-13] suggest a value close to 0.7. Successful applications of the standard BML model in stagnation flames have been reported by several authors [14,15]. If the mean spatial distribution of flamelet crossing points on the iso-$\bar{c}$ surface is exponential, g is taken to be 2.0 or if a symmetric beta probability distribution is assumed, a value of 1.0 may be taken. In practise, this distribution is found to vary in between symmetric and exponential range. Aluri *et al* [14] have used a value of 1.0 for g in Bunsen flame simulations, at the expense of tuning some of the other modal constants to match with experimental results. However, recent studies of Chew *et al* [16] and Patel & Ibrahim [17] show that scatter of crossing lengths are more biased towards an exponential distribution with an average g value of around 1.7-2.0. Further, they suggested that it would be better approximated for varying degree of reactions by $g = 1 + 2\bar{c}$, thus adopted here for the present study. l_i is the integral scale of turbulence and u' is the turbulent intensity for homogeneous isotropic turbulence. Using dimensional arguments, an expression can be derived for the integral scale of turbulence in isotropic homogeneous turbulence as;

$$l_i = \frac{c_\mu^{3/4}}{K}\frac{k^{1.5}}{\varepsilon} = c_l \frac{u'^3}{\varepsilon} \tag{3}$$

where c_μ and K are constants having the values 0.09 and 0.41 respectively. k is the turbulent kinetic energy and the ensemble proportionality constant c_l has an approximate value of 0.76.

C_b and n in Eq.(2) are model constants in the order of unity. Bray [18] proposed a value of 1.0 for n, though different fine-tuned values are found in the literature: for example, Aluri *et al* [14] recommended a value of 1.2. On the other hand, the scatter of model parameters C_b and n is so wide [11-18] and no reasonable mean value can be specified. This has become a major implication on standard BML model and all the above authors strongly suggest an alternative description for the flame wrinkling scale. In fact, Abu-Orf & Cant [9], Ranasinghe & Cant [19] and Watkins *et al* [8] have used alternative empirical correlations with the BML model in order to calculate the wrinkling scales in SI engine combustion.

Application of the standard BML model in wall-bounded systems is very rare. The reason behind this is the issue of wall flame acceleration: an inherent problem of this type of models. The BML relations initially proposed for the stagnation flames seem to severely over predict the burning rate near solid boundaries. Physically, this is unacceptable, as flames tend to extinguish at walls due to thermal quenching. BML model assumes isotropic turbulence. Thus, its application in the core region of the flame (where sufficiently homogeneous turbulent can be expected) provides satisfactory results. Conversely, near

solid boundaries, the homogeneous assumption is no longer valid, owing to the presence of a sharp gradient of turbulent properties. Furthermore, the turbulent intensity u' rapidly decreases towards zero, which eventually leads to very small values of the integral scale given by $l_i \sim u'^3/\varepsilon$. Consequently, the flame surface density becomes infinite, so as the reaction rate. To overcome this unphysical nature of the original BML model close to solid boundaries, alternative expressions have been proposed by Watkins *et al* [8], and Abu-Orf & Cant [9]. In these models, the flame wrinkling is assumed to be an empirical function of laminar flame thickness and the turbulent intensity. Necessary damping of the reaction rate near walls is artificially embedded via an exponential correlation. The fundamental disadvantage of these substitutions is that they neglect the well-known direct dependency of the integral scale on the flame wrinkling.

A DYNAMIC FORMULATION FOR THE FLAME WRINKLING SCALE

In the original process of derivation of the BML model constant n in Bray [18], the Kolmogorov – Pertovsky – Piskunow (KPP) analysis has been used where fractal combustion model was compared against the BML formulation. As this analysis was based on the assumption of homogeneous isotropic turbulence, its solution lead to the relation $n = 1$. In the case of wall-bounded systems like engines, where turbulent properties evolve in both the space and time, the validity of these assumptions is questionable. Hence, in a better combustion model, necessary allowance should be made to introduce the local anisotropy.

In this section, the turbulent flame speeds of BML model and the Fractal Flame combustion model (FFM) given by KPP analysis is evaluated. A new expression for the BML mode constant n is derived. Only the majors steps of the derivation are shown here and interested readers may refer to [20-23] for more details on KPP analysis. According to the KPP analysis, an expression for the turbulent burning velocity predicted by the BML model can be derived as:

$$S_{t,BML} = \sqrt{4C_{eff}u'I_0S_l\frac{g}{|\sigma_y|}\frac{1+\tau}{C_b\left(\frac{S_l}{u'}\right)^n}}$$ (4)

where $S_{t,BML}$ is the calculated turbulent flame speed by the BML model. Here τ is the heat release factor and the C_{eff} an ensemble constant. Using the fractal geometry an expression for the turbulent speed may be derived as:

$$S_{t,FFM} = C_tI_0'S_l\left(\frac{\epsilon_0}{\epsilon_i}\right)^{D-2}$$ (5)

Equating the turbulent velocities of both models yields:

$$C_tI_0'S_l\left(\frac{\epsilon_0}{\epsilon_i}\right)^{D-2} = \sqrt{4C_{eff}u'I_0S_l\frac{g}{|\sigma_y|}\frac{1+\tau}{C_b\left(\frac{S_l}{u'}\right)^n}}$$ (6)

In the early stage of fractal modelling the parameter C_t was considered to be a constant. However, later it was recognized that this would result in modelling deficiencies as shown by Gulder & Smallwood [24] and Zhao *et al* [25]. Therefore, C_t can be more accurately interpreted by assuming proportionality to $(u'/S_l)^{1/2}$, giving

$$C_t = C_t'\left(\frac{u'}{S_l}\right)^{1/2}$$ (7)

If the minimum and maximum scales of flame wrinkling is represented using the Gibson scale given by $l_G = S_l^3/\varepsilon$ and the integral scale respectively, the wrinkling scale becomes,

$$\left(\frac{\epsilon_0}{\epsilon_i}\right)^{D-2} = C_G^{D-2}\left(\frac{u'}{S_l}\right)^{3(D-2)}$$ (8)

Substituting Eqs.(6-8) the following final form is obtained.

$$C_t'I_0'C_G^{D-2}\left(\frac{u'}{S_l}\right)^{1/2}\frac{u'^{3(D-2)}}{S_l^{3D-7}}$$
$$= \sqrt{4C_{eff}I_0\frac{g}{|\sigma_y|}\frac{1+\tau}{C_b}\left(\frac{u'^{n+1}}{S_l^{n-1}}\right)}$$ (9)

By comparing the dimensions of both sides of the equation, it can be shown that:

$$n = 6D - 12$$ (10)

In Bray's original model [18], C_t was assumed to be a constant. The inner and outer flame wrinkling scales were assumed to be integral and Gibson scales respectively. This resulted in $n = 6D - 13$. Further, the fractal dimension was assumed to be a constant with a value $D = 7/3$ and this yields $n = 1$.

The advantage of our new formulation is that, for small values of u': such as in near walls, n reaches to zero, making the term $(S_l/u')^n$ term unity. For SI engine applications the fractal dimension is a variable. Complex nature of in cylinder combustion dynamics generates spatially and temporally varying flow properties. Thus, the use of a dynamic fractal dimension that can adjust itself according to in-cylinder conditions is essential. The relation suggested by Zhao *et al* [25], for the fractal dimension has such dynamic properties and used in the present modified BML model.

$$D = 2.05\frac{200}{200 + Re_t} + 2.35\frac{Re_t}{200 + Re_t}$$ (11)

One of the main contributions for the near wall singularity of the BML model is its use of classical definition of the integral scale to calculate the mean flame wrinkling scale given by Eq.(3). Initially, based on dimensional arguments, the above expression has been derived for isotropic turbulence. In contrast, for practical applications, corrections must be made to account for anisotropy.

In this regard, Sreenivasan's [26] work is brought to attention here. Several experimental data sets of grid generated turbulence length scales were compared in his study and a

functional dependence between the Taylor Reynolds number Re_λ and the turbulent integral scale constant c_l was found. Based on the observations of Sreenivasan [26], Lindsted and Vaos [27] obtained the following curve-fit correlation for c_l,.

$$c_l = 1 + \frac{a}{Re_\lambda} + \frac{b}{Re_\lambda^2} \qquad (12)$$

where a and b are constants having the values 5.715 and 72.051 respectively. This expression has been used in the present study for modelling the integral scale of turbulence. One of the main advantages of this expression is that it eliminates the singularity of the BML model at near zero turbulent intensities. Lindsted and Vaos [27] version of the BML model has shown to obtain comparable results in stagnation flame modelling at low Reynolds numbers.

FLAME QUENCHING AT SOLID BOUNDARIES

A flame front is quenched when it approaches a cold wall due to the excessive heat loss. In engine applications, it is believed that the unburned hydrocarbon formation is largely associated with wall quenching which results in partial burning of fuels. The quenching phenomenon is expected to be a chemically driven problem. Rate of quenching is determined by the relative intensity of heat release from combustion and the rate of absorption of heat by the cold boundary. One of the important recent findings on flame wall quenching is the identification of the existence of two distinct quenching regions. Closest to the wall, a total quenching region exists in which no reaction is ever taken place. Poinsot *et al* [28], through DNS data, estimated this length to be in correspondence to a quenching Peclet number of 3.5, where the Peclet number is defined as the ratio of the flame power to the wall heat flux. A simplified expression for the local Peclet number may be obtained as;

$$Pe = \frac{d}{\delta} \qquad (13)$$

where d is the distance from the wall and δ is the unstrained laminar flame thickness estimated based on dimensional arguments. In the region above the total quenching region: which is identified as the influence zone, the flame front senses the presence of the wall and is subjected to partial quenching. Estimated Peclet number corresponding to the distance for the outer boundary of the influence zone is in the in the order of 10.0 [28]. Gruber *et al* [29] have published more supporting evidence for the existence of two layers of quenching. Their DNS result indicates a total quenching zone thickness in the order of 3 flame thicknesses, while the influence zone is found be approximately 10 flame thicknesses. Poinsot *et al* [28] implemented their findings in the transport equation of equilibrium FIST model to modify the source term near solid boundaries. Their formulation is in the form of law of the wall model and the flame surface density in the first cell (which was assumed to be large enough so that the quenching zone is totally inside the cell) was appropriately modified via a simplified relation. Applied in engine combustion, it was found

to show a significant rate of reduction of flame surface density near solid boundaries.

Recent experimental investigations of Foucher *et al* [30] and Foucher & Russel [31] provide a new insight into the understanding of flame wall interaction. Laser tomographic images taken during head on wall quenching in an optical engine revealed the influence zone thickness could be as high as in the order of 40 times the quenching zone thickness, which is quite large compared to the DNS findings.
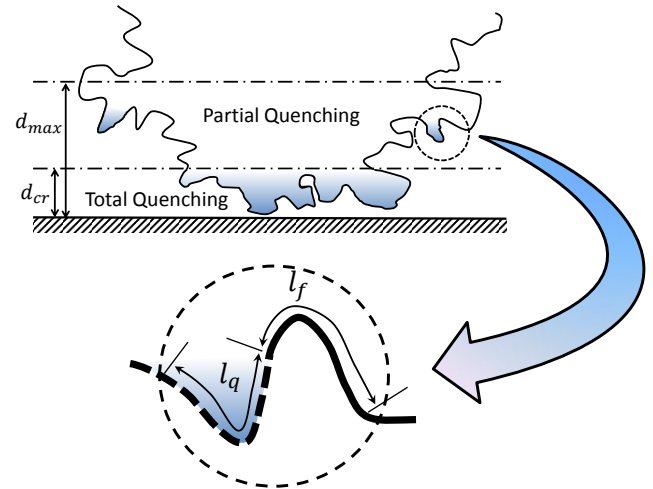
Figure 1 Two distinct zones, identified in flame wall quenching process. Exaggerated lengths of the reactive and quenched flame front in the partially quenched region are depicted in the dashed circle.

Foucher *et al* [31] extended their work in order to quantify their findings in Foucher *et al* [30] and using a fractal based method they were able to evaluate active flame surface area in the influenced zone. For this region, the quenching rate parameter QR has been defined as the ratio between the length of the active flame and the total flame length. Referring to Figure 1, this may be defined as;

$$QR = \frac{l_f}{l_f + l_q} \qquad (14)$$

where, l_f and l_q are respectively the active length and the quenched length of the flame front for a given length of the flamelet segment. Partial flame quenching also significantly results in reduced burning rates and incomplete burning of fuels. This suggests the necessity of introducing the wall-flame quenching effects into the burning rate integral in modeling studies. Foucher *et al* [31] experimentally verified that burning rate in the vicinity of a solid wall can be expressed in terms of the quenching rate as;

$$\bar{\bar{\omega}}_w = \rho_u\, I_0 S_l A_f \times QR \qquad (15)$$

where $\bar{\bar{\omega}}_w$ is the near wall unburned gas consumption rate. Evaluated quenching rates by Foucher *et al* [31] in head on quenching near the piston surface have been plotted in Figure 2.
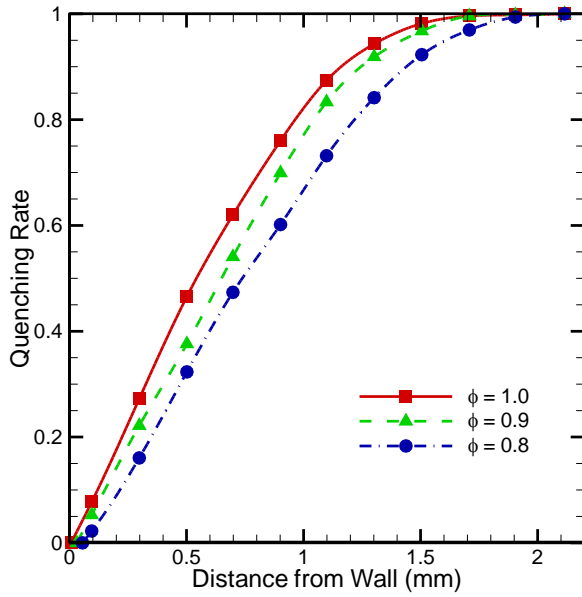
Figure 2 Calculated quenching rate vs the distance from solid wall for varying equivalence ratios. Adapted from Foucher *et al* [31]

The exhibited trend in variation of quenching rate with the distance from the wall for different air fuel ratios of methane air mixtures was found to be reasonably linear near the wall and then exponentially decay towards unity at the outer boundary of the influenced zone.

Foucher *et al* 's [31] estimation of QR was completely based on experimental observations and no mathematical formulation was presented to evaluate the quenching rate term. In order to implement their findings in a computer code a numerical formulation is needed. We have found that these results can be correlated quite remarkably with the following expressions.

Let, non-dimensional normalized distance $\mathcal{D}$ be taken as (Refer to Figure 2);

$$\mathcal{D} = \frac{(d - d_{cr})}{d_{max}} \tag{16}$$

$$0 \leq \mathcal{D} \leq 1 \tag{17}$$

where d is the distance measured from the solid wall, d_{cr} is the thickness of the total quenching zone and d_{max} is the distance to the outer boundary of the influenced zone. For physical and conceptual reasons the following limitations are imposed.

$$\mathcal{D} = 0 \ when \ d < d_{cr} \tag{18}$$

$$\mathcal{D} = 1 \ when \ d > d_{max} \tag{19}$$

Then the relation of QR vs $\mathcal{D}$ was found to show a similar trend seen previously with QR vs d. The above curves can be best fitted with the following relations.

$$QR = 1.0 - \frac{2.0}{1 + \exp(\mathcal{D})^{\alpha}} \tag{20}$$

$$\alpha = \frac{\beta}{(1.0 - 0.6\mathcal{D})} \tag{21}$$

$$\beta = 3.7 - 2|\varphi - 1.0| \tag{22}$$

Here β is the only parameter that varies with the operating conditions. Expression for β is arrived based on the assumption, that the minimum rate of quenching occurs at $\varphi = 1$. This assumption is valid as the variation of quenching Peclet number of many of the fuels is symmetric about the unity equivalence ratio or has only a small offset [32]. For much accurate calculations, a fuel specific determination of β is needed. However, due to the unavailability of experimental data, the trend shown in Foucher *et al*'s [31] analysis is assumed for all types of fuels used in the present study.
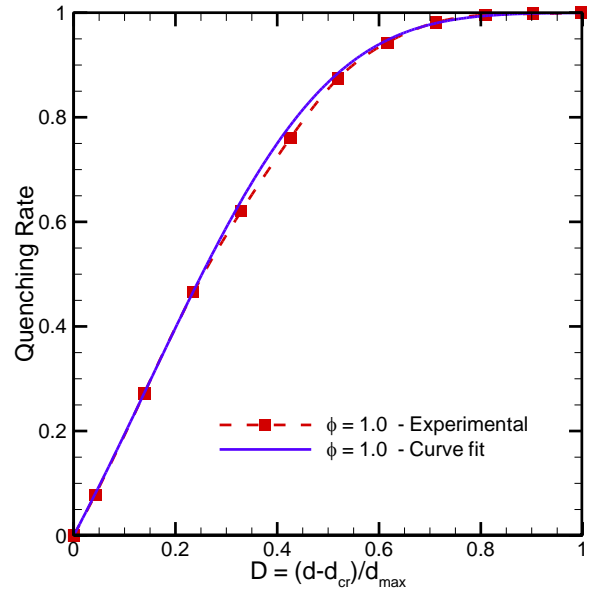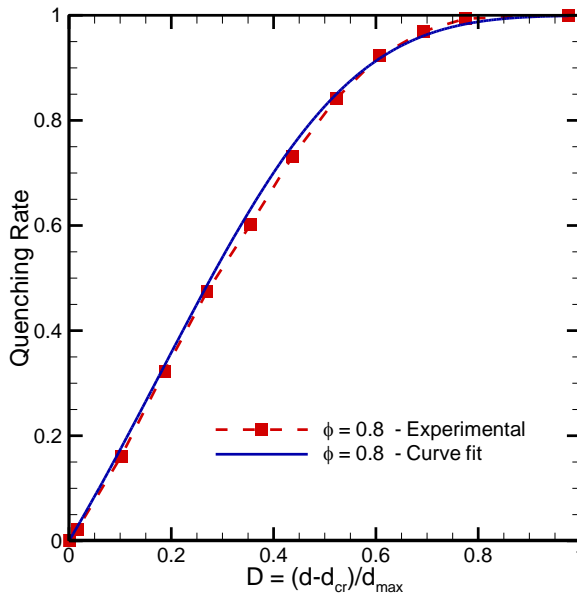

Figure 3 Experimental and curve fitted quenching rate for case 1: $\varphi = 1.0$ and $\beta = 3.7$

Figures 3-5 show the comparison of curve fitted graphs using the expression suggested by Eqs.(20-22), for the experimental cases considered. It can be seen that the agreement is remarkably good for the entire quenching zone thickness.

The usual practice in wall quenching studies is to represent the parameters in terms of the Peclet number. The region of interest, the quenching zone, is so small such that the variation of temperature, pressure and the other fluid properties can be negligible. This has been the basis of almost all the wall-quenching studies [32]. Under those assumptions, the laminar burning velocity and the kinematic viscosity of the fluid can also be considered constant and hence the laminar flame thickness (δ).
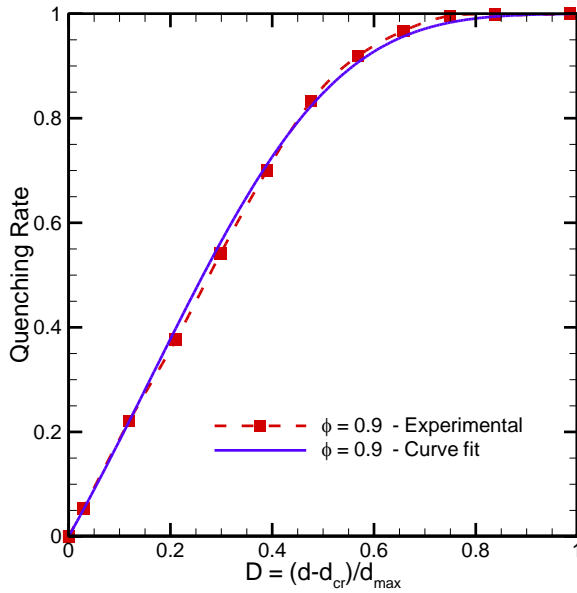
Figure 4 Experimental and curve fitted quenching rate for case 2: $\phi = 0.9$ and $\beta = 3.5$

Figure 5 Experimental and curve fitted quenching rate for case 3: $\phi = 0.8$ and $\beta = 3.3$

Normalizing of the wall distance d with respect to δ leads;

$$\mathcal{D} = \frac{(d - d_{cr})}{d_{max}} = \frac{\left(d/\delta - d_{cr}/\delta \right)}{d_{max}/\delta} \qquad (23)$$

Using Eq.(13), $\mathcal{D}$ is obtained in terms of the Peclet number.

$$\mathcal{D} = \frac{(Pe - Pe_{cr})}{Pe_{max}} \qquad (24)$$

The critical Peclet number is usually termed the quenching Peclet number in the literature and represented here by Pe_Q. Even though there have been many studies, a comprehensive mathematical formulation to evaluate the Peclet number at quenching conditions is yet to be found. The empirical expression used in this study is by Lavoie [33].

$$Pe_Q = \frac{1.9}{\phi} \left(\frac{p}{3} \right)^{0.26 \min(1, 1/\phi^2)} \qquad (25)$$

It should be noted here that this expression does not account for the effect of temperature variations in the quenching distances, which should essentially be embedded.

Only a limited number of research studies have been carried out to investigate the limits of maximum quenching distance. Among those, Foucher *et al* [30] and Fouchet & Rousselle [31] are the only experimental evidence for quenching distances in engine combustion. As the aim of the present study is to model the premixed combustion in SI engines, the maximum Peclet number is taken to be 40 times the quenching Peclet number as recommended by Foucher [30].

MODIFIED BML FORMULATION AND ITS VALIDATION

In this section, the application of the modified BML formulation with proposed improvements to model the combustion process in premixed combustion in SI engines are discussed. The final model form used in evaluating the unburned gas consumption rate is given by;

$$\bar{\omega} = \frac{C_{BML} \rho_r I_0 S_l}{|\sigma_y|} \frac{(1 + 2\bar{c})\bar{c}(1 - \bar{c})QR}{\left(1 + \dfrac{a}{Re_\lambda} + \dfrac{b}{Re_\lambda^2} \right) \dfrac{u'^3}{\varepsilon} \left(\dfrac{S_l}{u'} \right)^{6D-12}} \qquad (26)$$

where C_{BML} is the integrated model constant for the new version of the model. Flame stretching factor I_0 was modelled using the relation proposed by Bray[18]. The correlation of Gulder [34] was used to calculate the unstrained laminar burning velocity. No allowance was made to account the flame curvature effects assuming turbulent flame strain is predominant compared to its curvature counterpart.

The above model was then implemented in the new KIVA 4 CFD engine code [35], which is capable of solving the compressible Navier–Stokes equations in unstructured meshes with moving boundaries. Governing equations were solved in an Arbitrary Lagrnagian Eularian framework with standard $k - \varepsilon$ turbulence model. Iso-Octane was used as the combusting fuel in the present study. Fuel oxidisation is considered to be a simple one-step reaction and the reaction rate is calculated using the newly developed BML formulation. Early stage of the flame kernel was simulated using the popular Discrete Particle Ignition Kernel (DPIK) model and further information on this model can be found in Fan & Reitz [36].

As an initial validation of our new formulation, Propane combustion in the General Motor (GM) research engine published by Kuo and Reitz [37] was modelled. This engine has a pancake combustion chamber with a centrally located spark plug. Then the validation was extended to the modelling of full cycle combustion process in a Ricardo E6 single cylinder experimental engine tests at Loughborough University.

Specifications of E6 engine are given in the Table 1. Computational meshes for both cases comprised of unstructured hexahedron cells (Fig. 6). For both cases, the squish region contained around 100,000 computational cells, which corresponds to a cell dimension in the order of 1mm. Operating conditions of E6 engine are summarized in Table 2.

Table 1 Geometric details of Ricardo E6 engine

Bore (cm)	7.62
Stroke (cm)	11.11
Squish* (cm)	1.4428
Connecting Rod Length (cm)	24.13
Intake Valve Opening	009 - BTDC
Intake Valve Closing	217 - ATDC
Exhaust Valve Opening	147 - ATDC
Exhaust Valve Closing	010 - ATDC
Max. Intake Valve Lift (cm)	1.156
Max. Exhaust Valve Lift (cm)	1.06
Fuel	Gasoline

*Squish height is defined as the distance between piston crown surface and the cylinder head at piston TDC position

Table 2 Operating conditions of Ricardo E6 engine

Ricardo E6 engine : Fuel - Gasoline							
Case	φ	RPM	Spk. Ad. (BTDC)	Comp. Ratio	T_{in} (K)	T_w (K)	Fuel Mass (mg)
1	1.089	1500	16	8.7	298	360	425
2	0.967	1800	20	8.7	300	365	317
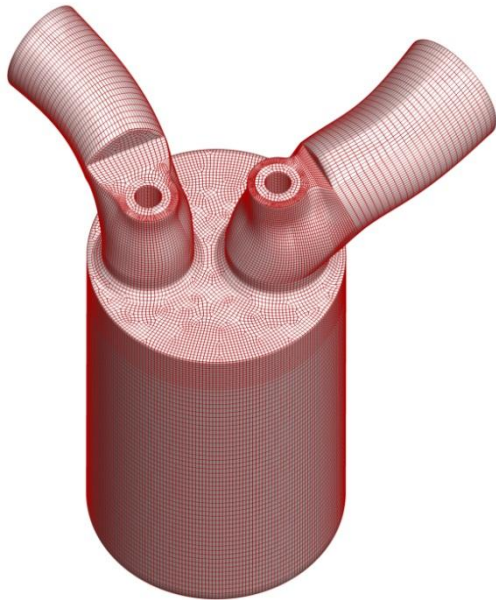
Figure 6 Computation mesh for Ricardo E6 engine simulations

Simulations of the Ricardo engine was started at 20 BTDC on exhaust stroke. Initial properties and mass fractions were calculated using a thermodynamic analysis. Based on exhaust gas temperature measurements, in cylinder and exhaust gas mixture temperatures of the Ricardo E6 engine were taken to be 750K at the start of simulation. In cylinder, fluid and turbulent properties were homogeneously initialized except the dissipation rate of turbulent kinetic energy, which was taken to be inversely proportional to the distance from the cylinder wall. Intake manifold pressure was slightly adjusted such that the trapped in-cylinder air and fuel masses were equal to the measured quantities.
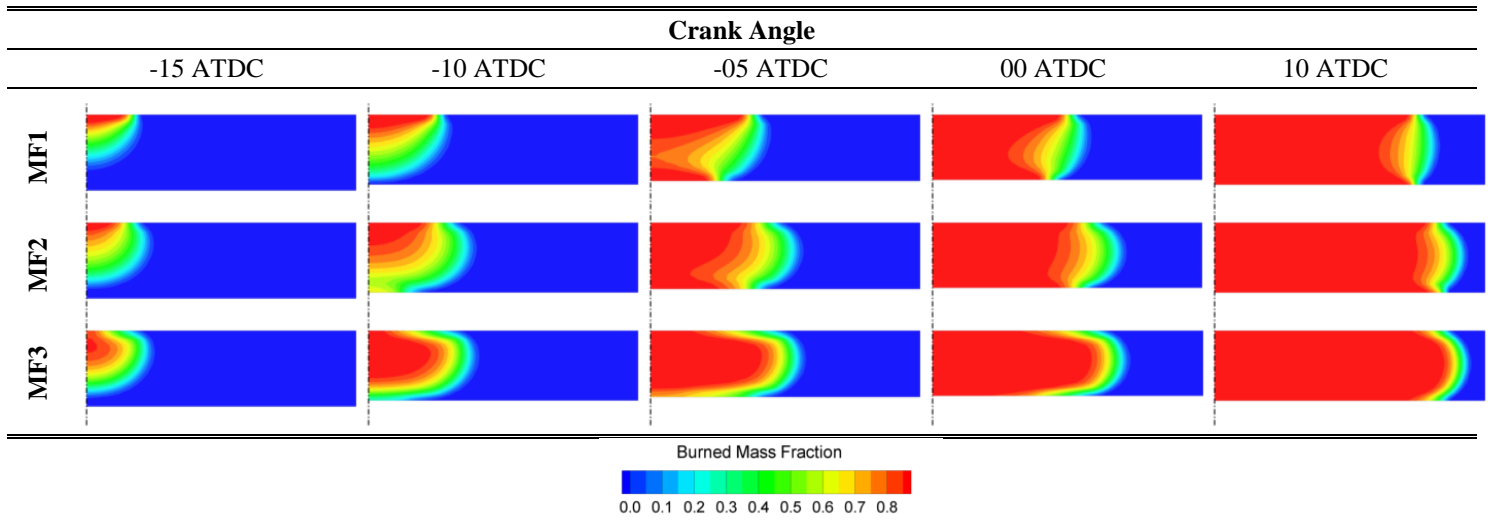
RESULTS AND DISCUSSION

One of the main objectives of the present study is to investigate the suitability of the present improved BML model in predicting wall-bounded combustion. Thus, the propagation of flame in the vicinity of solid walls in the General Motors research engine [37] was examined with the aim of assessing the effects of each of the suggested improvements. As a reference case, the standard BML model (MF1) with classical definition for the integral scale and constant $n = 1$ was used and the resultant flame evolution is shown in the first row of Figure 7. The second row depicts the prediction of the new BML model without the wall-quenching model (MF2). Illustrated in the third row is the complete model results, which comprises of dynamic calculation of model constants and the quenching model (MF3).

Figure 7 shows the variation of burned mass fraction of fuel across an axial cross section plane in the engine cylinder with the crank angle. Reacting zone may be identified as the region between zero and unit fuel mass fraction. Zero represents the unburned zone and unity is for the fully burned zone. When the burned mass fractions are close to unity near walls, the excessive flame acceleration with the standard BML (MF1) model is apparent even from the very early stage of the combustion process. This is more noticeable in the figure corresponding to -5ATDC where the burned fuel fraction reaches unity much faster on the piston surface even before the core area reaches its maximum. As a result, the propagating flame front is seen to be concave in the inner region and nearly flat in the leading front, where in reality both these regions are observed to be convex.

Introduction of the dynamic calculation of model constants (MF2) has made a considerable improvement over the standard model and has resulted in a more physical convex and outward flame front. However, in the vicinity of the walls a comparatively high rate of reaction can still be seen. Dynamic evaluation of model constants with the allowance for local anisotropy has made a big improvement over MF1, but at walls u' becomes so small such that it overcomes the damping of dynamically calculated c_l and n.

As can be seen in the third row, employment of the novel quenching correlation (MF3) has been able to successfully hinder the flame wall acceleration and has made the flame front agreeably convex. In addition, the flame brush thickness is also has made thinner than the other model forms, which is more acceptable in this type of low turbulence engines. This observations are in good agreement with the optical imaging results of Weller et al [7].

Next, the results from the full cycle engine simulation of Ricardo E6 engine are discussed. Illustrated in Figure 8 is the in cylinder flow structure of this engine at the end of the intake period. Non-uniform complex velocity field with an eddy structure centred below the intake valve and the bulk tumble motion of the charge air mixture can clearly be seen. This bulk flow motion has a major effect on the early flame kernel formation.

	-15 ATDC	-10 ATDC	-05 ATDC	00 ATDC	10 ATDC
MF1					
MF2					
MF3					

Burned Mass Fraction

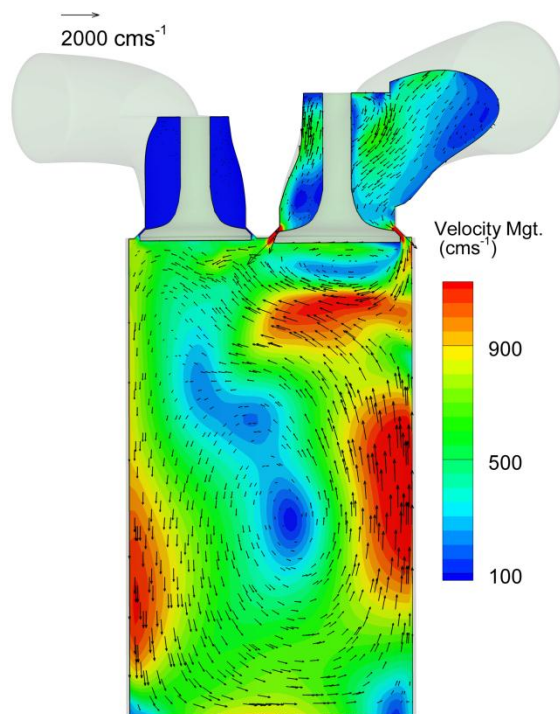0.0 0.1 0.2 0.3 0.4 0.5 0.6 0.7 0.8

Figure 7 Propagation of the turbulent flame front represented using the burned fuel mass fraction in the GM research engine combustion chamber.
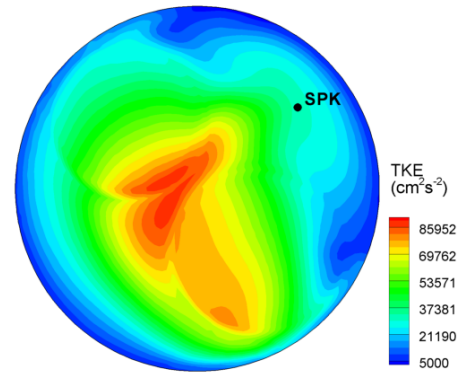
The emerging kernel is convected away from the spark location by the surrounding flow motion so that the centre of the turbulent flame is essentially locates away from the spark location. These effects can be accounted only in a full cycle simulation, where the evolution of the flow filed is modelled right from the beginning.

The turbulent flow field in the vicinity of the spark plug shown in Figure 9 appears less intense compared to the core region of the cylinder. This would verify that the assumption of 'spherical flame kernel assumption' made in the DPIK model is valid for the present test cases of Ricardo E6 engine

2000 cms^{-1}

Velocity Mgt. (cms^{-1})

900

500

100

Figure 8 Distribution of the flow velocity field in Ricardo E6 engine for case 1, 20 CAD after the bottom dead centre of the intake stroke, across the intake valve plane

One of the main characteristics of turbulence, decaying towards solid boundaries, can also be identified from the Figure 9. The near wall intensity of the turbulent kinetic energy is within the range 0-5000 $cm^2 s^{-2}$, which is approximately about 15 times than the core region value. Hence, the conventional approach of BML model should result in flame wall acceleration when applied to this test case

•SPK

TKE (cm^{2}s^{-2})

85952
69762
53571
37381
21190
5000

Figure 9 Turbulent kinetic energy profile on the spark location plane at 344 CAD

In the application of the new BML model, C_{BML} was set to 2.15 for all the test cases. Pressure trace predictions are compared with the experimentally measured values and shown in Figures 10 and 11. In general, the predicted and simulated traces of in cylinder pressure are in good agreement. The model has precisely captured the trends in in-cylinder pressure variation for different engine operating conditions. Estimation of the peak pressure was reasonably accurate. Predicted peak pressure locations are slightly deviated by few crank degrees within the range of 0- 4 degrees.

It is noted that the model over predict the pressure trace during the last stage of exhaust stroke. This may probably be due to the absence of a blow by model in the present study. In the first case where there is a higher peak pressure and a lower engine speed, the over prediction is much apparent compared

to the second case where engine speed is higher and the peak pressure is low. In the second case, as less time and a lower peak pressure is available less blow by mass is expected, so that the predictions closely follows the experimental trace. In general, the overall agreement in the pressure predictions during the early and middle stage of the engine cycle is quite satisfactory for both cases indicating the success in combustion predictions.
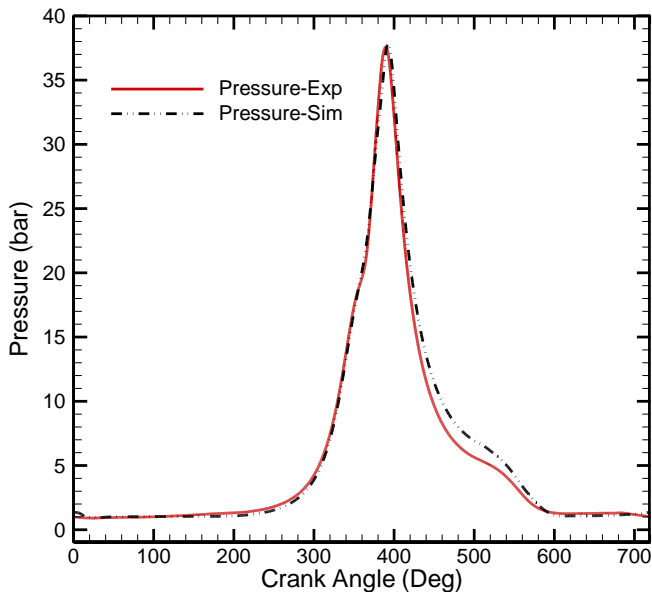
Figure 10 Comparison of measured and predicted in-cylinder pressure: case 1
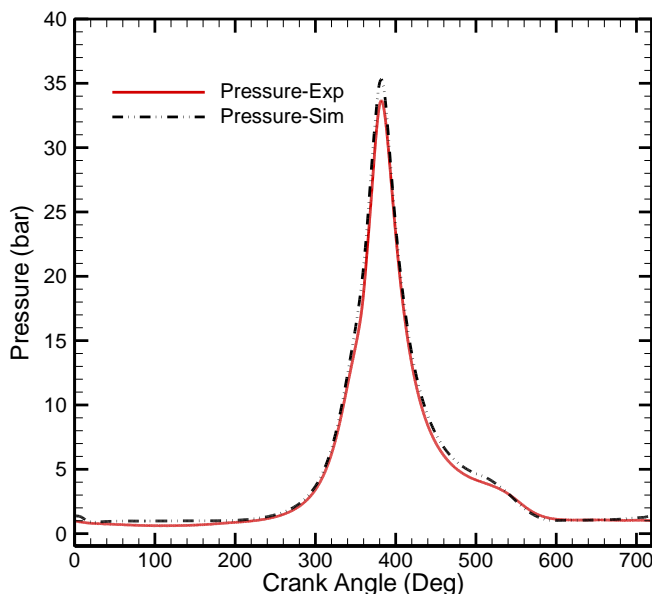
Figure 11 Comparison of measured and predicted in-cylinder pressure: case 2

CONCLUSIONS

Standard BML model involves several adjustable model constants. It also produces poor results when applied to wall bounded combustion modeling, due to flame wall acceleration problem.

A new comprehensive model based on the classical BML model was developed with capability of evaluating most of the model constants dynamically. Further improvements were made so that it can also be applied to wall bounded combustion simulations. A new empirical correlation was derived to account the wall flame quenching effects on reaction rate.

The new model formulation was then tested for predicting premixed combustion in SI engines. Classical BML model was found to unrealistically high reaction rates near solid walls. Simulations shows that the new model successfully captured the expected and experimentally observed flame front evolution. It has the capability of accurately calculating the near wall reaction rates eliminating the wall flame acceleration problem seen in previous model variations. The proposed quenching rate model has also shown to predict better results. Full cycle engine simulations with the improved version of the BML model shows that modified model satisfactorily predicted the experimentally observed pressure data.

REFERENCES

[1] Pinchón P., Modelling of fluid dynamics and combustion in piston engines, *International Symposium COMODIA*, 1990

[2] Vincent M., Barton I., Angelberger C., and Poinsot T., Towards large eddy simulation in internal-combustion engines: simulation of a compressed tumble flow, *SAE Paper 2004-01-1995*, 2004

[3] Magnussen B.F., Hjertager B.H., On mathematical modelling of turbulent combustion with special emphasis on soot formation and combustion. *Sixteenth Symposium (International) on Combustion*. Comb. Inst., Pittsburg, Pennsylvania, 1976, pp.719-729

[4] Spalding B., Development of the eddy-break-up model of turbulent combustion, *Symposium (International) on Combustion*, Volume 16, 1977, pp. 1657-1663

[5] Marble F.E., and Broadwell J.E., The coherent flame model for turbulent chemical reactions, *Technical Report : TRW-9-PU*, Project Squid, 1977

[6] Henson J.C., and Malalasekera W., Full-cycle firing simulation of a pent-roof spark-ignition engine with visualization of the flow structure, flame propagation and radiative heat flux, *Proceedings of the Institution of Mechanical Engineers. Part D: Journal of engineering,* Vol.214, 2000, pp. 957-971

[7] Weller H.G., Uslu S., Gosman A.D., Maly R.R., Herweg R. and Heel B. Prediction of combustion in homogeneous-charge spark-ignition engines, *International Symposium COMODIA*, 1994

[8] Watkins A.P., Li S.P. and Cant R.S. Premixed Combustion Modelling for Spark engine Applications, *SAE Paper : 961190*, 1996

[9] Abu-Orf G.M., and Cant R.S., A turbulent reaction rate model for premixed turbulent combustion in spark ignition engines, *Combustion and Flame*, Vol. 252, 2000, pp. 122-133

[10] Bray K.N.C., Chmapion M., and Libby P.A., The interaction between turbulent and chemistry in premixed turbulent flames, *In Turbulent Reacting Flows (Borghi R. and Murthy S.N.B., Eds)*, *Springer Verlag,* Berlin, 1989, pp.541-563

[11] Chang N.W., Shy S.S., Yang S.I. and Yang T.S. Spatially resolved flamelet statistics for reaction rate modelling using premixed methane-air flames in a near-homogeneous turbulence, *Combustion and Flame*, Vol.127, 2001, pp. 1880 - 1894

[12] Lahjaily H., Champion M., Karmed D., and Bruel P., Introduction of dilution in the BML model: application to a stagnating turbulent flame, *Combustion Science and Technology*, Volume 135, 1998, pp.153-173

[13] Shy S.S., Jang R.H., I W.K., and Gee K.L., Three dimensional spatial flamelet statistics for premixed turbulent combustion modelling, *Twenty-Sixth Symposium (International) on Combustion*, The Combustion Institute, 1996, pp.283-289

[14] Aluri N.K., Pantangi P.K.G., Muppala S.R.P. and Dinkelacker A numerical study promoting algebraic models for the Lewis number effect in atmospheric turbulent premixed Bunsen flames, *Flow Turbulence and Combustion,* Vol.75, 2005, pp.149-172.

[15] Bailly P., Garreton D., Simonin O., Bruel P., Champion M., Deshaies B., Duplantier S., and Sanquer S., Experimental and numerical study of a premixed flame stabilized by a rectangular section cylinder, *Twenty-Sixth Symposium (International) on Combustion*, The Combustion Institute, 1996, pp.923-929.

[16] Chew T.C., Bray K.N.C., and Britter R.E., Spatially resolved flamelet statistics for reaction rate modelling, *Combustion and Flame,* Vol. 80, Issue 1, 1990, pp. 65–82

[17] Patel S.N.D.H., and Ibrahim S.S., Calculations of burning velocity of turbulent premixed flames using a flame surface density model, *JSME International Journal*, series – B, Vol. 45, 2002, pp.725-735

[18] Bray K.N.C., Studies of the turbulent burning velocity, *Proceedings of the Mathematical and Physical Science*, Vol.431, 1990, pp. 315-335

[19] Ranasinghe J., and Cant R.S., A Turbulent combustion model for a stratified charged, spark ignited internal combustion engine, *SAE Paper*: 2000-01-0275, 2000

[20] Hackberg M., and Gosman A.D., Analytical determination of turbulent flame speed from combustion models, *Twentieth Symposium (International) on Combustion*, The Combustion Institute, 1984, pp. 225-232

[21] Fichot F., Lacas F., Veynante D., and Cnadel S., One dimensional propagation of a premixed turbulent flame with a coherent flamelet model, *Combustion Science and Technology,* Vol. 89, 1993, pp.1-26

[22] Duclos J.M., Veynante D., and Poinsot T., A Comparison of flamelet models for premixed turbulent combustion, *Combustion and Flame*, Vol.95, 1993, pp.101-117

[23] Poinsot T., and Veynante D., *Theoretical and numerical combustion*, Edwards, 2001,ISBN: 1-930217-05-6

[24] Gülder Ö.L., and Smallwood G.J., Do Turbulent premixed flame fronts in spark-ignition engines behave like passive surfaces?, *SAE Paper* :2000-01-1942, 2000

[25] Zhao X., Matthews R.D., and Ellzey J.L., Numerical simulations of combustion in si engines: comparison of fractal flame model to the coherent flame model, *International Symposium COMODIA*, 1994

[26] Sreenivasan K.R., On the Scaling of the turbulent energy dissipation rate, *Physics of Fluids*, Vol. 27,1984, pp. 1048-1051

[27] Lindstedt R.P., and Váos E.M., Modelling of premixed turbulent flames with second moment methods, *Combustion and Flame*, Volume 116, 1999, pp. 461–485

[28] Poinsot T.J., Haworth D.C., and Bruneaux G., Direct simulation and modelling of flame-wall interaction for premixed turbulent combustion. *Combustion and Flame,* Vol 95, 1993, pp.95-118

[29] Gruber A., Sankaran R., Hawkes E.R. and Chen J. H., Turbulent flame–wall interaction: a direct numerical simulation study, *Journal of fluid mechanics,* Vol.658,2010, pp.5-32

[30] Foucher F., Brunel S., and Rousselle M., Evaluation of burning rates in the vicinity of the piston in a spark-ignition engines, *Proceedings of the Combustion Institute,* Vol.29, 2002, pp.751-757

[31] Foucher F., and Rousselle M., Fractal approach to the evaluation of burning rates in the vicinity of the piston in a spark-ignition engine. *Combustion and Flame*, Vol.143, 2005, pp.323-332

[32] Karrer M., Bellenoue M., Labuda S., Sotton J., and Makarov M., Electrical probe diagnostics for the laminar flame quenching distance, *Experimental Thermal and Fluid Science,* Vol. 34,2010, pp. 131-141.

[33] Lavoie G.A., Correlation of combustion data for SI engine calculations − laminar flame speed, Quenching distance and global reaction rate, *SAE Paper : 780229*, 1978

[34] Gülder Ö.L., Correlation of laminar combustion data for alternative SI engine fuels. *SAE Paper* : 841000,1984

[35] Torres D.J., and Trujillo M.F., KIVA-4: An unstructured ale code for compressible gas flow with sprays, *Journal of Computational Physics*, Vol.216, 2006, pp.943-975

[36] Fan L., and Reitz R.D., Development of an ignition and combustion model for spark-ignition engines, *SAE Paper*: 2000-01-2809, 2000

[37] Kuo T.W., and Reitz R.D., Computation of premixed-charge combustion in pancake and pent-roof engines, *SAE Paper : 890670*,1989